

Impact of Component Sizing in Plug-In Hybrid Electric Vehicles for Energy Resource and Greenhouse Emissions Reduction¹

Andreas A. Malikopoulos

Energy & Transportation Science Division,
Oak Ridge National Laboratory,
Knoxville, TN 37932
e-mail: andreas@ornl.gov

Widespread use of alternative hybrid powertrains currently appears inevitable and many opportunities for substantial progress remain. The necessity for environmentally friendly vehicles, in conjunction with increasing concerns regarding U.S. dependency on foreign oil and climate change, has led to significant investment in enhancing the propulsion portfolio with new technologies. Recently, plug-in hybrid electric vehicles (PHEVs) have attracted considerable attention due to their potential to reduce petroleum consumption and greenhouse gas (GHG) emissions in the transportation sector. PHEVs are especially appealing for short daily commutes with excessive stop-and-go driving. However, the high costs associated with their components, and in particular, with their energy storage systems have been significant barriers to extensive market penetration of PHEVs. In the research reported here, we investigated the implications of motor/generator and battery size on fuel economy and GHG emissions in a medium duty PHEV. An optimization framework is proposed and applied to two different parallel powertrain configurations, pretransmission and post transmission, to derive the Pareto frontier with respect to motor/generator and battery size. The optimization and modeling approach adopted here facilitates better understanding of the potential benefits from proper selection of motor/generator and battery size on fuel economy and GHG emissions. This understanding can help us identify the appropriate sizing of these components and thus reducing the PHEV cost. Addressing optimal sizing of PHEV components could aim at an extensive market penetration of PHEVs. [DOI: 10.1115/1.4023334]

Keywords: optimization methods, transportation, vehicles, emissions, energy storage

1 Introduction

1.1 Motivation. Hybrid electric vehicles (HEVs) have shown the potential to achieve greater fuel economy than vehicles powered only by internal combustion (IC) engines (conventional vehicles) [1–6]. This capability is mainly attributable to (1) the potential for downsizing the engine, (2) the potential for recovering energy during braking and thus recharging the energy storage unit, and (3) the ability to minimize the operation of the engine in inefficient brake specific fuel consumption regimes. In addition, hybridization of conventional powertrain systems allows elimination of near idle engine operation and thus enables direct fuel economy enhancement [3,4]. A typical HEV powertrain configuration consists of the fuel converter (engine), the electric machines (motor and generator), the energy storage system (battery), the torque coupler, and the transmission. Depending on the driving mode (e.g., cruising or braking), either a positive or a negative torque is demanded from the engine. The power available from the electric machine is regulated by adjusting its torque such that it can be ei-

ther positive or negative depending on the operating mode as designated by the power management control algorithm. In the motor mode, the electric machine contributes power to the driveline by drawing electrical energy from the energy storage unit. In the generator mode, the electric machine absorbs power from the driveline and charges the energy storage unit. In cruising, positive power is demanded at a fixed torque and speed. In braking, negative torque is applied by the electric machine (e.g., generator), which absorbs the maximum possible amount of energy imposed by generator and battery constraints. Above this limit, brake friction is required to convert any excess kinetic energy to heat.

The automotive industry has recognized that widespread use of alternative hybrid powertrains is currently inevitable and many opportunities for substantial progress remain [7]. The necessity for environmentally conscious vehicle designs in conjunction with stringent emissions regulations has led to significant investment in enhancing the propulsion portfolio with new technologies. Recently, PHEVs have attracted considerable attention [8]. PHEVs are hybrid vehicles with rechargeable batteries that can be restored to full charge by connecting a plug to an external electric wall socket. A PHEV shares the characteristics of both an HEV, having an electric motor and an IC engine, and an all-electric vehicle, having a plug to connect to the electrical grid. It is especially appealing in situations where daily commuting is over short distances [9]. Studies have shown that about 60% of U.S. passenger vehicles travel less than 30 miles each day [10]. However, the high costs associated with their energy storage systems have been significant barriers to extensive market penetration of PEVs. The research presented here aims at enhancing the understanding of

¹This manuscript has been authored by UT-Battelle, LLC, under contract DE-AC05-00OR22725 with the U.S. Department of Energy. The U.S. government retains and the publisher, by accepting the article for publication, acknowledges that the U.S. government retains a nonexclusive, paid-up, irrevocable, worldwide license to publish or reproduce the published form of this manuscript, or allow others to do so, for U.S. government purposes.

Contributed by the Internal Combustion Engine Division of ASME for publication in the JOURNAL OF ENERGY RESOURCES TECHNOLOGY. Manuscript received September 20, 2012; final manuscript received December 18, 2012; published online May 27, 2013. Assoc. Editor: Timothy J. Jacobs.

the impact of motor/generator and battery size of a PHEV on fuel economy and GHG emissions. This understanding can help us identify the right sizing of these components, and thus reducing the PHEV cost. Addressing optimal sizing of PHEV components could aim to an extensive market penetration of PHEVs.

1.2 Literature Overview. PHEVs have the potential to reduce petroleum consumption and greenhouse gas (GHG) emissions by means of sophisticated control schemes. State-of-the-art research and development and future trends in the modeling, design, control, and optimization of energy-storage systems for electric vehicles, HEVs, fuel cell vehicles, and PHEVs were presented in Ref. [11]. Moreover, a detailed review and classification of current control strategies for PHEVs are provided in Ref. [12].

Under the average mix of electricity sources in the United States, PHEVs can be driven with lower operating costs and fewer GHG emissions per mile when powered by electricity rather than by gasoline [13]. Most PHEVs on the road today are passenger cars, but there are also PHEV versions of commercial vehicles, utility trucks, buses, and military vehicles. Realizing the optimal size and operation of the motor, generator, and battery in HEVs and PHEVs is essential. Guzzella and Amstutz [14] presented a tool to support the systematic design and optimization procedures in HEVs with the aim of realizing the optimal parameterization and power management control among the subsystems (e.g., motor, generator, battery, and engine). Wang et al. [15] formulated an optimization problem for minimizing fuel consumption in PHEVs with respect to the size of the energy storage system. Sung Chul Oh [16] developed dynamic models for electric motors to analyze several HEVs through hardware-in-the-loop. Inoa and Wang [17] studied efficient charging strategies of a Li-ion battery intended for PHEVs. Tara et al. [18] developed a simulation-based optimization framework to realize the optimal sizing of the energy storage system in HEVs and PHEVs.

Various optimization approaches focusing on minimizing fuel consumption and emissions in hybrid vehicles with respect to component sizing and powertrain architecture have been reported in the literature. Previous research efforts include the optimization study conducted by Triger et al. [19] to identify the optimal engine size in an HEV. Aceves et al. [20] demonstrated the gain in fuel economy by optimizing two series hybrid concept vehicles, one operating with a stoichiometric engine and the other with a lean-burn engine. Moore [21] utilized a set of five linked spreadsheets to size powertrain components based on continuous and peak power demand. Zoelch and Schroeder [22] employed dynamic optimization to compute optimal engine torque, electric motor torque, and transmission gear ratios for a parallel HEV. Assanis et al. [23] demonstrated an optimization framework for the design of a parallel hybrid electric system for a midsize passenger car, linking a high fidelity engine model with the overall vehicle system. Fellini et al. [24] presented a modular simulation and design environment where optimization algorithms can be utilized to study a variety of hybrid powertrain configurations. Recently, Shiau et al. [25] presented an optimization model integrating vehicle simulation polynomial metamodels, battery degradation data, and U.S. driving data; the proposed model identifies optimal vehicle designs and allocation of vehicles to drivers for minimum net life-cycle cost, GHG emissions, and petroleum consumption under a range of scenarios. Yusaf [26] determined the optimum operation conditions for a diesel engine used as a hybrid power unit. Crane and Bell [27] presented a design concept that maximizes the performance for thermoelectric power generation systems in which the thermal power to be recovered is from a fluid stream subject to varying temperatures and a broad range of exhaust flow rates.

Optimizing the design of a hybrid vehicle is tightly coupled with the power management control algorithm [28]. The latter determines the power split demanded by the driver between the thermal (engine) and electrical paths (electric machine and energy storage

unit). Bumbay and Forster [29] used a direct search technique to obtain an optimal control by minimizing the energy path through the driving cycle with respect to the torque split and gear ratio controllable variables. The optimized control was followed by parametric studies to optimize component size. Capata and Lora [30] presented a power management unit for a low emissions turbo hybrid electric vehicle in conjunction with the components of the propulsive system. Filipi et al. [31] proposed a method for the combined optimization of design and power management for a hydraulic hybrid Class VI truck. The method establishes a sequential optimization framework suitable to yield an optimal solution fulfilling a given vehicle's mission. Another simultaneous optimization of HEV component sizing and control strategy was presented in Ref. [32] through a multiobjective self-adaptive differential evolution algorithm; the intention of this work was to provide a set of Pareto optimal solutions. Nino-Baron et al. [33] proposed an optimization algorithm to determine the torque and speed reference signals for the engine-generator subsystem that achieve maximum efficiency in a series HEV. Syed et al. [34] proposed a nonlinear proportional-integral controller using the fuzzy control paradigm for a power-split HEV to achieve improved engine speed behavior. Martinez et al. [35] introduced a control strategy to manage the energy in an HEV by using fuzzy logic. Sezer et al. [36] developed the equivalent consumption minimization strategy for series HEVs by simultaneously facilitating the optimization of fuel consumption and multiple emission components.

The research objective here and in related work by the author [37] was to investigate the impact on fuel economy and GHG emissions of varying the size of two key PHEV components (motor/generator and battery). In this paper, we propose an optimization framework that has implications for motor/generator and battery size in a medium duty PHEV. Our approach utilizes a set of polynomial metamodels, which are constructed as functions of the key design variables of interest. The polynomial construction facilitates analytical investigation of trends and reduction of computation times. We apply this approach to two different parallel powertrain configurations, pretransmission and post transmission, and derive the optimal design with respect to motor/generator and battery size. Finally, we compare the fuel economy and GHG emissions potentials of conventional and PHEV configurations with equivalent size and performance under the same driving conditions.

The remainder of the paper proceeds as follows. In Sec. 2, we summarize the steps required to model the conventional and two PHEV parallel configurations in *Autonomie*. In Sec. 3, we describe the development of a set of polynomial metamodels that reflect the influence of our key design variables (motor/generator and battery size) and propose our optimization framework. In Sec. 4, we present optimization results and analysis from our simulations, and in Sec. 5, we present overall conclusions.

2 Vehicle System Modeling

For the evaluation of various vehicle performance indices required for our optimization study, we employed *Autonomie* [38]. *Autonomie* is a MATLAB/SIMULINK simulation package for powertrain and vehicle model development developed by Argonne National Laboratory. With a variety of existing forward-looking powertrain and vehicle models, *Autonomie* can support the evaluation of new technologies for improving fuel economy through virtual design and analysis in a math-based simulation environment.

This particular medium duty vehicle was intended for a specific duty cycle representative of typical operation that corresponds to the JE-05 driving cycle, illustrated in Fig. 1. Consequently, the two PHEV parallel configuration models were subjected to this cycle. To utilize the full energy storage potential of the energy storage system, the vehicle models were run over nine consecutive JE-05 cycles. Thus, both full charge-depleting (CD) and charge-sustaining (CS) operation were achieved.

Three basic powertrain configurations were analyzed as part of this study and are summarized in Tables 1 and 2. For each

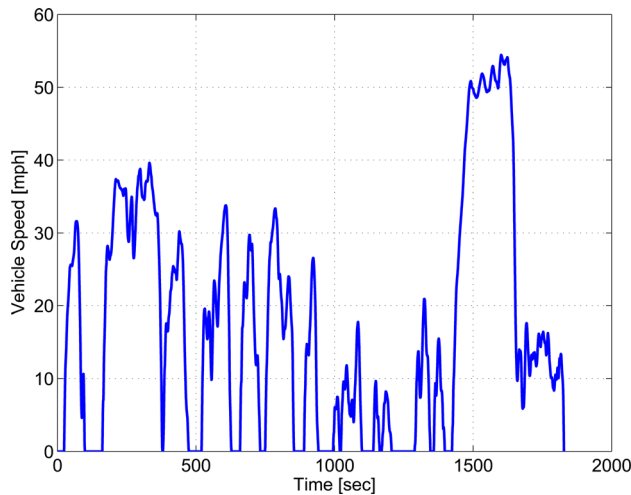


Fig. 1 Japanese driving cycle

Table 1 Vehicle specification

	Description	Characteristics
Vehicle	Mass	14,969 kg
	Body length	10.36 m
	Frontal area	6.32 m ²
	Coefficient of drag	0.65
Engine	Configuration	V8
	Displacement	6.4L
	HP	230
	Torque	312 nm
	Rated speed	2800 rpm
	Operating torque speed	1400–1800 rpm
Transmission	Dry weight	556 kg
	1st gear ratio	3.51
	2nd gear ratio	1.9
	3rd gear ratio	1.44
	4th gear ratio	1
	5th gear ratio	0.74
	6th gear ratio	0.64
	Reverse	5.09
Torque converter (TC)	TC stall torque ratio	1.91
Starter	Power	25 kW

Table 2 Plug-in hybrid electric vehicle component specifications

	Description	Characteristics
Battery	Nominal capacity	41 Ah
	Nominal voltage	3.6 V
	Maximum charging/discharging rate	C/5
	Number of cells in series per module	118
	Number of cells in parallel per module	1
	Energy per module SOC operating range	5.2 kWh 80%–20%
Motor/generator	Range of continuous power used	60–120 kW
Final drive	Ratio	5.57
Torque converter (TC)	TC stall torque ratio	1.91
Reduction gear	Ratio	2.13

respective powertrain variant, certain components were kept constant. Table 1 outlines all of the common components present in each powertrain configuration, including the conventional vehicle. Table 2 outlines common powertrain components utilized only for the pretransmission and post transmission parallel PHEV architectures.

We adopted a blended supervisor control strategy that uses a mix of the electric motor and engine to power the vehicle in CD mode. For all the PHEV simulations, the state of charge (SOC) of the vehicle was allowed to fluctuate with a delta SOC of 60% (80% initial SOC depleting to 20% SOC). Certain constraints were placed on the control strategy for the desired operation of the vehicle: (a) the powertrain had to operate as an all-electric vehicle below vehicle speeds of 25 mph during CD operation and (b) the engine had to turn on at vehicle speeds greater than 45 mph for drivability reasons.

2.1 Conventional Configuration. A conventional powertrain was implemented to serve as a point of reference. The conventional vehicle features a basic two-wheel drive configuration with automatic transmission and torque converter. Standard transmission shift schedules based on accelerator pedal position (driver demand) and current vehicle speed were used.

2.2 Pretransmission Parallel Configuration. The pretransmission parallel configuration builds on the conventional architecture by adding a high voltage traction drive and energy storage system at the interface of the engine. In this implementation, the torque converter is replaced by a clutch, and the motor/generator is used for speed matching during shifts. Thus, this configuration resembles an operation with automated manual transmission. One potential advantage of this architecture over the post transmission variant is that vehicle idle charging is possible. If this vehicle is subjected to long periods of idle, then turning the engine on and charging can easily replenish the SOC of the energy storage system.

2.3 Post Transmission Parallel Configuration. The post transmission parallel configuration builds on the conventional architecture by coupling a high voltage traction drive and energy storage system between the transmission and final drive. This is necessary to fully realize the operating envelope of the traction motor and ensure the performance of this variant is not compromised over the prescribed drive cycle. During all-electric operation, the transmission is shifted into neutral so that drag torque from the engine is avoided. One benefit of this architecture over the pretransmission variant is regenerative braking efficiency is maximized as a result of the physical location of the traction motor.

It is important to note that because the PHEV variants of the standard powertrain configuration retain all of the baseline components (e.g., transmission, final drive, engine, chassis, and wheels), it is expected that during highway operation the fuel efficiency of the PHEV will most likely be slightly less than the conventional vehicle due to the mass penalty imposed by the addition of the high voltage traction components.

3 Optimization Framework

To formulate the optimization problem analytically and reduce computation time, a set of polynomial metamodels was constructed to reflect the responses produced by changes in the design variables (e.g., motor/generator and battery size). Although neural networks can also be used for the evaluation of the objective function and constraints, with the use of polynomial metamodels, we can express the problem analytically and get a better understanding about the tradeoffs between fuel economy and emissions with respect to the size of the motor/generator and battery. A metamodel is a model of a model, which is used to approximate a usually

expensive analysis or simulation process; metamodeling refers to the techniques and procedures to construct such a model [39]. In our optimization framework, a set of polynomial metamodels was used to express the objective function and the constraints. In particular, fuel economy, GHG emissions, and 0–30 mph and 0–60 mph acceleration times were evaluated through simulation in Autonomie over a grid of values for motor/generator and battery sizes. Then multivariate polynomial functions were fit to the data using least squares.

3.1 Regression Model. The least squares method is a fundamental approach for parameter estimation. If the model has the property of being linear in the parameters then the least squares estimate can be calculated analytically [40]. We assume that the model, we wish to identify is in the form

$$\hat{y}(i) = \varphi_1(i) \cdot \alpha_1 + \varphi_2(i) \cdot \alpha_2 + \dots + \varphi_n(i) \cdot \alpha_n \quad (1)$$

where $i = 1, 2, \dots, n, n \in \mathbb{N}$ indexes the number of simulation data points; \hat{y} is the output of the model; $\alpha_1, \alpha_2, \dots, \alpha_n$ are the parameters of the model to be determined; and $\varphi_1, \varphi_2, \dots, \varphi_n$ are known functions that may depend on other known variables. The model in Eq. (1) can be written in the vector form as follows:

$$\hat{y}(i) = \boldsymbol{\varphi}^T(i) \cdot \boldsymbol{\alpha} \quad (2)$$

where $\boldsymbol{\varphi}^T(i) = [\varphi_1(i) \ \varphi_2(i) \ \dots \ \varphi_n(i)]$ and $\boldsymbol{\alpha} = [\alpha_1 \ \alpha_2 \ \dots \ \alpha_n]^T$. The model in Eq. (1) is the regression model, and the functions $\varphi_i, i = 1, 2, \dots, n$ are called the “regression variables.” The simulation data points derived from Autonomie correspond to pairs of the measured and regression variables $\{(y(i), \boldsymbol{\varphi}(i)), i = 1, 2, \dots, n, n \in \mathbb{N}\}$. The problem is formulated so as to minimize the following least squares cost function with respect to the parameters of the model $\alpha_1, \alpha_2, \dots, \alpha_n$:

$$R(\boldsymbol{\alpha}, n) = \frac{1}{2} \sum_{i=1}^n [y(i) - \hat{y}(i)]^2 = \frac{1}{2} \sum_{i=1}^n [y(i) - \boldsymbol{\varphi}^T(i) \cdot \boldsymbol{\alpha}]^2 \quad (3)$$

The measured variable y is linear in parameters α_i , and the cost function is quadratic. Consequently the problem admits an analytical solution. Let \mathbf{Y} and $\hat{\mathbf{Y}}$ be the vector of the measured variables and output of the model, respectively

$$\mathbf{Y} = [y(1), y(2), \dots, y(n)]^T \quad (4)$$

and

$$\hat{\mathbf{Y}} = [\hat{y}(1), \hat{y}(2), \dots, \hat{y}(n)]^T \quad (5)$$

and let \mathbf{E} be the vector of the error $e(i)$ between the measured variable and output of the model

$$\mathbf{E} = [e(1), e(2), \dots, e(n)]^T \quad (6)$$

where $e(i) = y(i) - \hat{y}(i) = y(i) - \boldsymbol{\varphi}^T(i) \cdot \boldsymbol{\alpha}$. Substituting Eq. (6) in Eq. (3), the cost function can be written as

$$\boldsymbol{\varphi}^T(i) = [x_1^3(i) \ x_2^3(i) \ x_1^2(i) \cdot x_2(i) \ x_1(i) \cdot x_2^2(i) \ x_1^2(i) \ x_2^2 \ x_1(i) \cdot x_2(i) \ x_1(i) \ x_2 \ 1] \quad (12)$$

where x_1 and x_2 are the design variables. The range of values for the motor/generator size, x_1 , used to derive the simulation data points in continuous power is $x_1 = \{60, 80, 100, 120\}$ kW. Similarly, the range of values for the battery size in number of

$$R(\boldsymbol{\alpha}, n) = \frac{1}{2} \sum_{i=1}^n e(i)^2 = \frac{1}{2} \|\mathbf{E}\|^2 \quad (7)$$

Our objective is to derive the vector of the model parameters $\boldsymbol{\alpha}$ that makes the error be equal to zero, that is

$$\mathbf{E} = \mathbf{Y} - \hat{\mathbf{Y}} = \mathbf{Y} - \boldsymbol{\Phi} \cdot \boldsymbol{\alpha} = 0 \quad (8)$$

where $\boldsymbol{\Phi}(n) = [\boldsymbol{\varphi}^T(1) \ \boldsymbol{\varphi}^T(2) \ \dots \ \boldsymbol{\varphi}^T(n)]^T$. Consequently, the solution of the least squares problem is given by solving Eq. (8)

$$\begin{aligned} \mathbf{Y} &= \boldsymbol{\Phi} \cdot \boldsymbol{\alpha} \Leftrightarrow \\ \boldsymbol{\Phi}^T \cdot \mathbf{Y} &= \boldsymbol{\Phi}^T \cdot \boldsymbol{\Phi} \cdot \boldsymbol{\alpha} \Leftrightarrow \\ (\boldsymbol{\Phi}^T \cdot \boldsymbol{\Phi})^{-1} \cdot \boldsymbol{\Phi}^T \cdot \mathbf{Y} &= (\boldsymbol{\Phi}^T \cdot \boldsymbol{\Phi})^{-1} \cdot (\boldsymbol{\Phi}^T \cdot \boldsymbol{\Phi}) \cdot \boldsymbol{\alpha} \Leftrightarrow \\ \boldsymbol{\alpha} &= (\boldsymbol{\Phi}^T \cdot \boldsymbol{\Phi})^{-1} \cdot \boldsymbol{\Phi}^T \cdot \mathbf{Y} \end{aligned} \quad (9)$$

If the matrix $\boldsymbol{\Phi}^T \boldsymbol{\Phi}$ is nonsingular, then the solution of Eq. (9) is a unique minimum for the least squares problem [40].

3.2 Optimization Objective Function and Constraints. In our optimization problem formulation, the vector of the design variables \mathbf{x} consists of the motor/generator size, x_1 , and the battery size, x_2 . The set of polynomial metamodels is a function of the vector \mathbf{x} . A cubic fitting function of the following form provides an appropriate fitting to the discrete simulation data points [39] for the PHEV performance indices (1) fuel economy, $f_{\text{fuel economy}}(\text{mpg})$; (2) GHG emissions, f_{CO_2} (kg-CO₂); (3) 0–30 mph acceleration time, t_{0-30} (s); and (4) 0–60 mph acceleration time, t_{0-60} (s)

$$\begin{aligned} f(x_1, x_2) &= a_1 x_1^3 + a_2 x_2^3 + a_3 x_1^2 x_2 + a_4 x_1 x_2^2 + a_5 x_1^2 + a_6 x_2^2 \\ &\quad + a_7 x_1 x_2 + a_8 x_1 + a_9 x_2 + a_{10} \end{aligned} \quad (10)$$

To identify the appropriate order of polynomial metamodel that fits the discrete simulation data points well, the norm of residuals given by the following was used

$$\|r\| = \left(\sum_{i=1}^n (y(i) - \hat{y}(i))^2 \right)^{1/2} \quad (11)$$

The norm of residuals for each model corresponding to the PHEV performance indices were plotted against the order of the polynomial metamodel, as shown in Figs. 2–5. In all cases, a third order polynomial yields the smallest value of the norm of residuals, and a higher order does not seem appropriate to fit the simulation data.

The polynomial coefficients of the regression model used for each of the output values to fit a set of discrete simulation data points over a grid of values were derived using least squares. The vector of known functions, $\boldsymbol{\varphi}^T$, in Eq. (10) is

modules is $x_2 = \{6, 7, 8, 9, 10\}$, each of which includes 118 cells in series and 1 cell in parallel (Table 2). As a result, the simulation data set is created over a grid of 20 different inputs (i.e., $i = 1, 2, \dots, 20$).

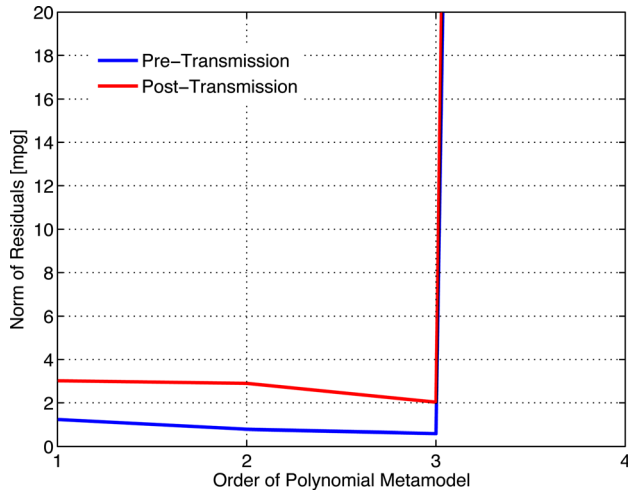


Fig. 2 Norm of residuals of the polynomial metamodel for fuel economy versus the order of the polynomial

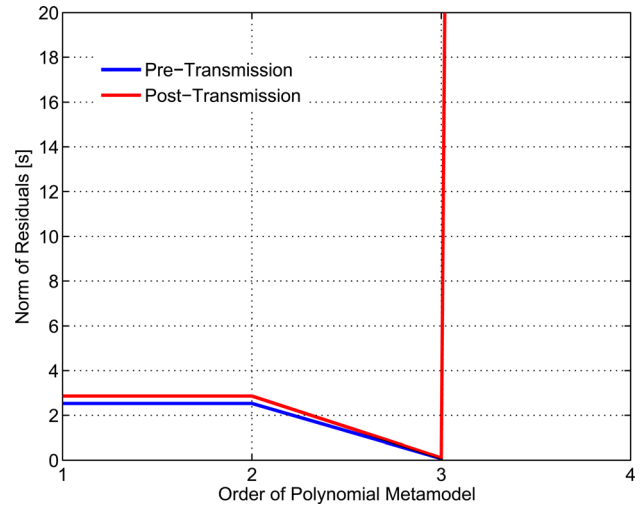


Fig. 5 Norm of residuals of the polynomial metamodel for an acceleration time of 0-60mph versus the order of the polynomial

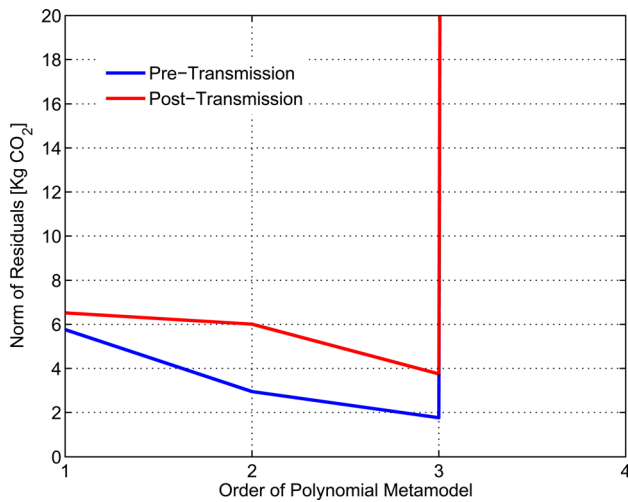


Fig. 3 Norm of residuals of the polynomial metamodel for greenhouse gas emissions versus the order of the polynomial

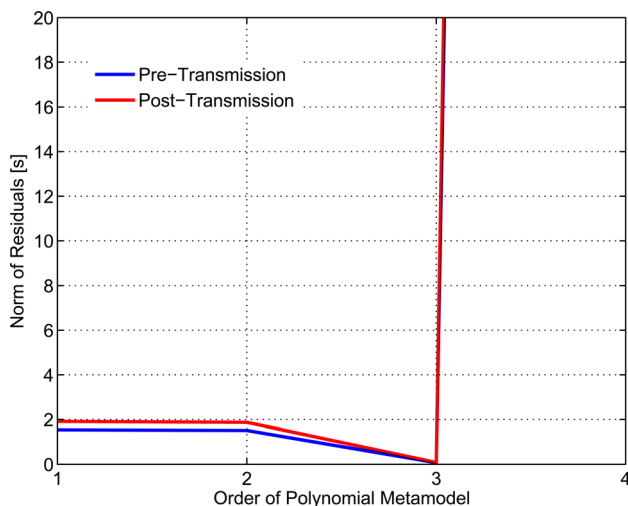


Fig. 4 Norm of residuals of the polynomial metamodel for an acceleration time of 0-30mph versus the order of the polynomial

3.2.1 Fuel Consumption. The amount of fuel consumed by each vehicle for the nine consecutive JE-05 driving cycles is computed directly by Autonomie. Autonomie also provides the values of fuel economy, $f_{\text{fuel economy}}$, in miles per gallon.

3.2.2 Greenhouse Gas Emissions. The average GHG emissions, f_{CO_2} , in kilograms of CO₂ (kg-CO₂) for the nine consecutive JE-05 cycles are associated with the amount of CO₂ corresponding to the diesel and electricity portions. Consequently, given the fuel efficiency, η_{fuel} (mpg), and electricity efficiency, η_E (miles/kWh), derived from simulation in Autonomie, the average GHG emissions are computed by the following equation:

$$f_{\text{CO}_2} = s \cdot \left(\frac{N_{\text{CO}_2}^D}{\eta_{\text{fuel}}} + \frac{N_{\text{CO}_2}^E}{\eta_E} \cdot \frac{1}{\eta_{\text{BC}}} \right) \quad (13)$$

where $s = 77$ miles is the distance driven by the vehicle over the nine consecutive JE-05 driving cycles, $N_{\text{CO}_2}^D = 10.1$ kg-CO₂/gal for diesel life-cycle emissions [41], $N_{\text{CO}_2}^E = 0.752$ kg-CO₂/kWh for electricity emissions [42,43], and $\eta_{\text{BC}} = 88\%$ for battery charging efficiency [43].

3.2.3 Acceleration Performance Metrics. For the 0-30 mph and 0-60 mph acceleration times, t_{0-30} (s) and t_{0-60} (se), we performed simulated tests in CS mode in Autonomie. Using the discrete simulation data points from Autonomie derived over the input grid described above, we computed the polynomial fitting coefficients, α , for each regression model (i.e., $f_{\text{fuel economy}}$, f_{CO_2} , t_{0-30} , and t_{0-60}) by solving Eq. (9) using Eq. (12).

Tables 3 and 4 give the resulting values of polynomial coefficients and the values of the norm of residuals for each regression model, which provide a good indication that the regression models fit the data well.

3.3 Optimization Problem Formulation. The purpose of the optimization framework established here is to determine the impact of the vector of the design variables, \mathbf{x} , consisting of the motor/generator size, x_1 , and battery size, x_2 , on both fuel economy and GHG emissions. This framework was applied in the optimization study to determine which one of the two PHEV configurations was more efficient in terms of fuel economy and GHG emissions.

For each PHEV configuration, a multiobjective optimization problem was investigated consisting of two functions: (1) fuel economy and (2) GHG emissions. The objective was to maximize

Table 3 Polynomial coefficients of the PHEV pretransmission parallel configuration metamodels

	$f_{\text{fuel economy}}$	f_{CO_2}	t_{0-30}	t_{0-60}
a_1	0.0000	0.0000	0.0001	0.0002
a_2	-0.0777	0.2992	-0.0042	-0.0042
a_3	0.0002	-0.0002	0.0000	0.0000
a_4	0.0026	-0.0154	0.0001	-0.0002
a_5	-0.0020	0.0046	-0.0312	-0.0527
a_6	1.5362	-5.1994	0.0894	0.1283
a_7	-0.0717	0.2676	-0.0015	0.0038
a_8	0.4407	-1.3995	2.6316	4.4511
a_9	-7.5871	26.6705	-0.4871	-0.9371
a_{10}	16.3026	60.3627	-51.7722	-80.5970
$\ r\ $	0.59	1.76	0.07	0.07

Table 4 Polynomial coefficients of the PHEV post transmission parallel configuration metamodels

	$f_{\text{fuel economy}}$	f_{CO_2}	t_{0-30}	t_{0-60}
a_1	-0.0002	0.0004	0.0001	0.0002
a_2	-0.0004	-0.0287	0.0063	-0.0042
a_3	0.0002	-0.0003	0.0000	0.0000
a_4	0.0078	-0.0151	-0.0001	0.0001
a_5	0.0428	-0.0962	-0.0389	-0.0596
a_6	-0.8028	2.7026	-0.1368	0.0911
a_7	-0.1314	0.2487	-0.0008	-0.0029
a_8	-3.3305	7.6294	3.2825	5.0467
a_9	13.4367	-35.0972	1.2736	-0.2285
a_{10}	69.6121	-38.2324	-71.6626	-96.8739
$\ r\ $	2.03	3.75	0.08	0.10

fuel economy and minimize GHG emissions with respect to the vector of the design variables, \mathbf{x} , subject to the acceleration performance metrics corresponding to values deemed characteristic of this type of vehicle. Thus, the mathematical problem consists of the following multiobjective function and constraints:

$$\min_{\mathbf{x}} \left(w_1 \cdot \frac{1}{f_{\text{fuel economy}}(\mathbf{X})} + w_2 \cdot f_{\text{CO}_2}(\mathbf{X}) \right) \quad (14)$$

subject to $t_{0-30} \leq 15 \text{ sec}$
 $t_{0-60} \leq 55 \text{ sec}$

where w_1 and w_2 are the weighting factors of the objective function. It turned out that the constraints are not active since the size of the engine can provide the required power to satisfy the acceleration performance criteria. Fuel economy and GHG emissions in Eq. (14) are normalized to avoid dominance of one function over the other. To study the impact of the motor/generator and battery size and the associated trade-offs between fuel economy and GHG emissions, a general quantitative Pareto-based assessment was constructed by varying the weighting factors from 0 to 1. This assessment aims to identify the optimal motor/generator and battery size considering the associated trade-offs of fuel economy and GHG emissions.

In multiobjective optimization the focus is on the explicit trade-offs between competing criteria. The objective is to find a Pareto point and define the preference structure for selecting one point among many.

The general vector optimization problem is formulated as

$$\min_{\mathbf{x}} f_m(\mathbf{x}; \mathbf{w})$$

subject to $g_i(\mathbf{x}; \mathbf{w}) \leq 0, \quad i = 0, \dots, m \quad (15)$
 $h_j(\mathbf{x}; \mathbf{w}) = 0, \quad j = 0, \dots, p$

where $\mathbf{x} \in \mathbb{R}^n$ is the vector of the optimization variables, $w \in \mathbb{R}^n$ is the set of weighting factors, $f_m : \mathbb{R}^n \rightarrow \mathbb{R}^q$ is the multiobjective function, $g_i : \mathbb{R}^n \rightarrow \mathbb{R}$ are the inequality constraints, and $h_j : \mathbb{R}^n \rightarrow \mathbb{R}$ are the equality constraints. The set of objective values of feasible points

$$S := \{f_m(\mathbf{x}; \mathbf{w}) | \exists \mathbf{x} \in \mathbb{R}^n, g_i(\mathbf{x}; \mathbf{w}) \leq 0, i = 1, \dots, m, h_j(\mathbf{x}; \mathbf{w}) = 0, \times j = 1, \dots, p\} \subseteq \mathbb{R}^q \quad (16)$$

is defined as the set of *achievable objective values*. If this set has a minimum element \mathbf{x}^* , then it is said that this point is optimal for the problem formulated in Eq. (15), and refer to $f_m(\mathbf{x}^*)$ as the *optimal value* of the problem. In the vector optimization problems where the set of achievable objective values does not have a minimum element, the minimal elements of the set of achievable values play an important role. A feasible point \mathbf{x} is Pareto optimal if $f_m(\mathbf{x}^*)$ is a minimal element of the set of achievable values S . The set of minimal elements of S is called the Pareto frontier; namely, given a set of feasible values of the objective function, the Pareto frontier (or Pareto set) is the set of feasible values that are Pareto efficient.

4 Optimization Results and Analysis

The impact of varying the motor/generator and battery size on fuel economy in PHEV pretransmission and post transmission parallel configurations is illustrated in Figs. 6 and 7. Increasing the battery size has a significant impact on fuel economy, partly attributable to the additional amount of electricity from grid that can be stored and used to power the vehicle. The motor/generator size, on the other hand, impacts fuel economy only in conjunction with a larger battery size. The combination of a large motor/generator and large battery enhances energy recovery during brake regeneration. This is more apparent in the PHEV post transmission configuration, where fuel economy is noticeably improved.

Increasing the battery size has some interesting implications for GHG emissions. For architectures with small motor/generators, increasing the number of modules in the battery is not beneficial for GHG emissions. On the contrary, a moderate number of modules seems to be the optimal battery size for both configurations, as illustrated in Figs. 8 and 9. For a large motor/generator, the impact of a large battery is quite different for the pretransmission and post transmission configurations. For the PHEV pretransmission configuration, GHG emissions are minimal for a combination of a 120 kW motor/generator with a six-module battery. For the PHEV post transmission configuration, on the other hand, a 120 kW motor/generator in combination with a battery with 10 modules seems to be the optimal solution for GHG emissions. Although by increasing the battery size the contribution in GHG emissions from the electricity grid is also increased Eq. (13), this is compensated by the enhanced capability in the post transmission configuration to store energy from brake regeneration.

For the PHEV pretransmission configuration it seems that there is a trade-off between fuel economy and GHG emissions in the multiobjective optimization problem formulated in Eq. (14), shown in Figs. 6 and 8. To understand the trade-off better we need to look at the Pareto frontier of the multiobjective function, illustrated in Fig. 10. Clearly, maximizing fuel economy and minimizing GHG emissions simultaneously is not possible. The optimal motor/generator and battery size corresponding to each value in the Pareto frontier is illustrated in Fig. 11. It seems that the optimal motor/generator size is 120 kW, while the battery size has an impact on the Pareto solution. By increasing the battery size fuel economy is increased (the inverse of fuel economy is decreased in Fig. 10 by sacrificing GHG emissions. Although the optimization with respect to the motor/generator and battery size was conducted in the continuous domain, it should be emphasized that the final selection of the size of these components will be based on the nearest discrete available values.

The multiobjective optimization problem formulated in Eq. (14) has an apparent visual solution for the PHEV post transmission

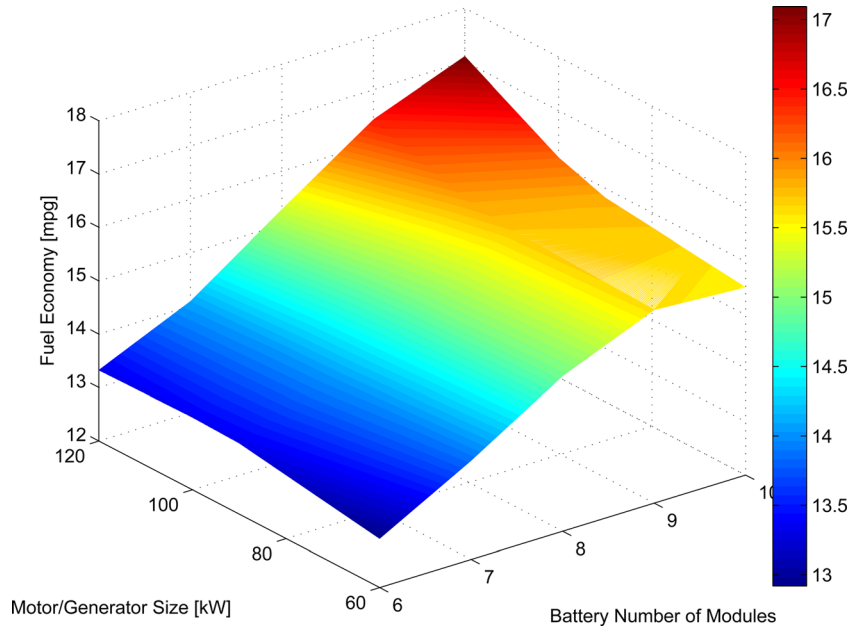


Fig. 6 Fuel economy variation in PHEV pretransmission configuration

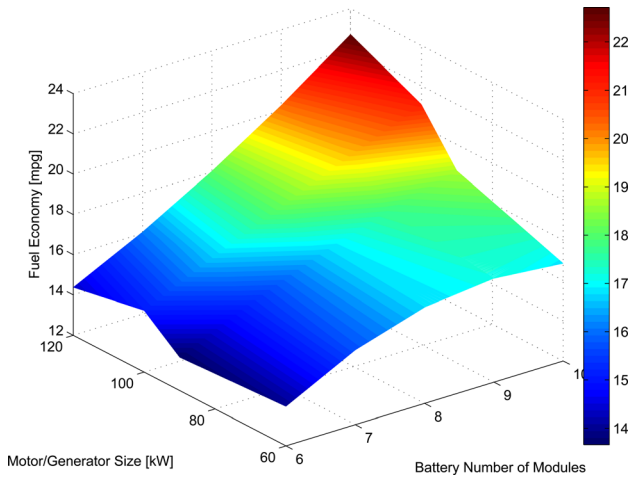


Fig. 7 Fuel economy variation in PHEV post transmission configuration

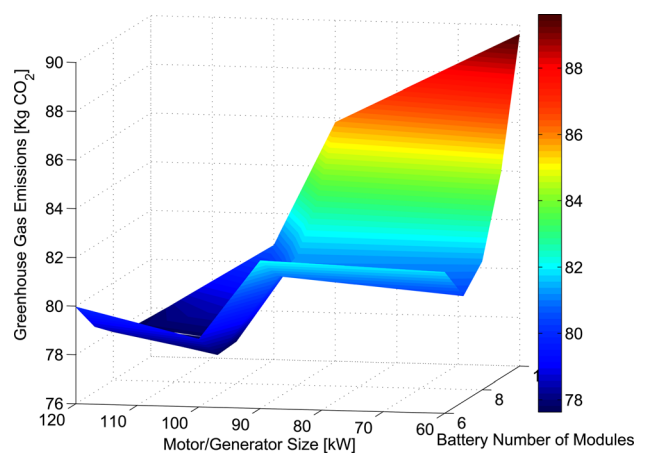


Fig. 9 GHG emissions in PHEV post transmission configuration

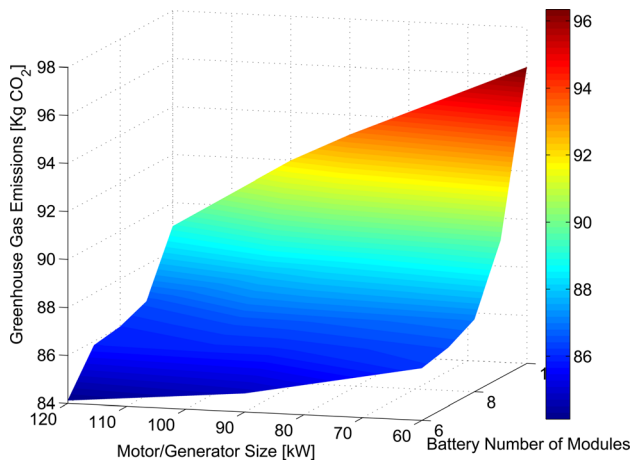


Fig. 8 GHG emissions in PHEV pretransmission configuration

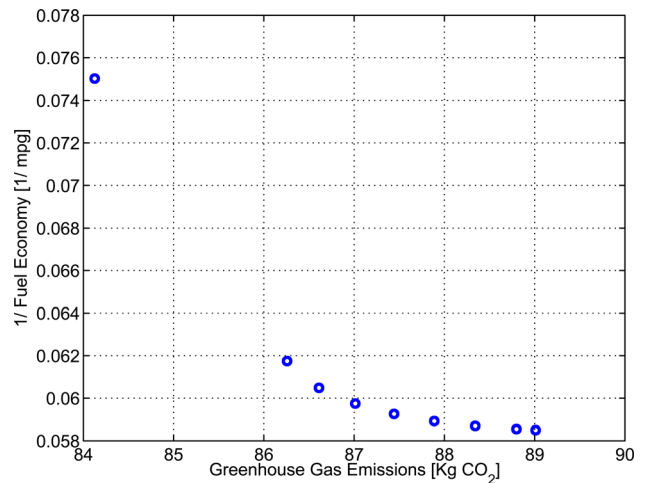


Fig. 10 Pareto frontier in PHEV pretransmission configuration

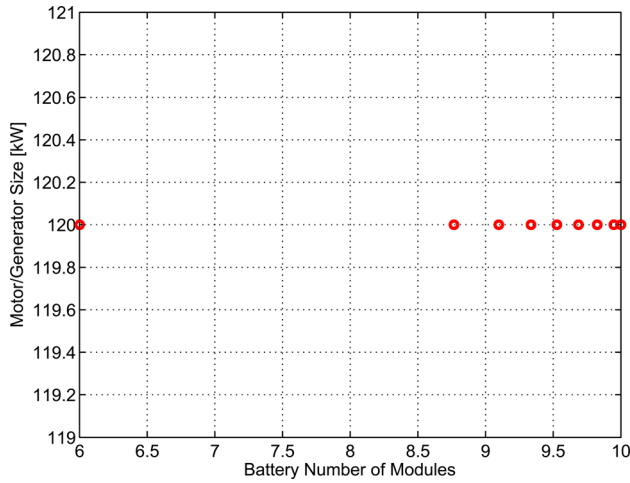


Fig. 11 Optimal set of the motor/generator and battery size corresponding to the Pareto frontier in the PHEV pretransmission configuration

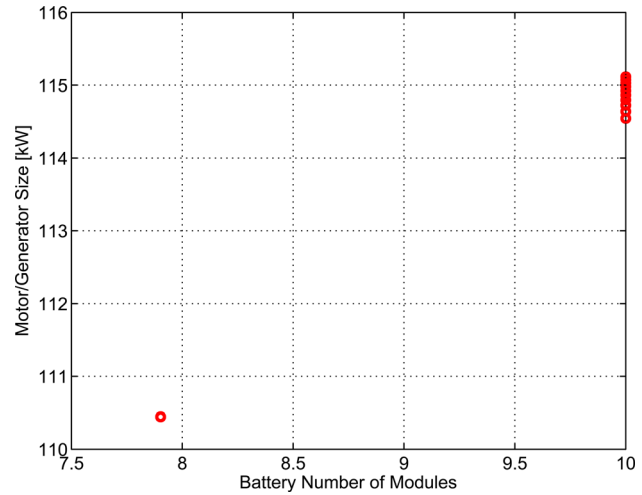


Fig. 13 Optimal set of the motor/generator and battery size corresponding to the Pareto frontier in the PHEV post transmission configuration

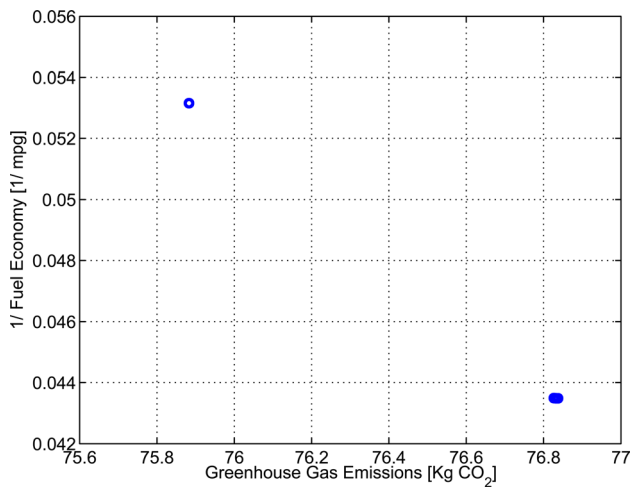


Fig. 12 Pareto frontier in PHEV post transmission configuration

configuration, as shown in Figs. 7 and 9; namely, the optimal solution for both fuel economy and GHG emissions is a big motor/generator with a 10-module battery. This is also apparent from the Pareto frontier and the optimal motor/generator and battery size corresponding to the Pareto frontier, illustrated in Figs. 12 and 13. A combination of a big motor/generator size (about 115 kW) with a 10-module battery is the optimal solution because it enhances energy recovery during brake regeneration deemed characteristic in the post transmission PHEV configuration as a result of the physical location of the motor/generator. Especially for the battery, the biggest possible size is the optimal solution in order to absorb all possible energy recovery during brake regeneration. The single Pareto efficient value in the plots corresponds to the case when only GHG emissions are considered in Eq. (14) (i.e., the weighting factors w_1 and w_2 are equal to 0 and 1, respectively).

Increasing the motor/generator and battery sizes has, as might be expected, an impact on the vehicle mass (depicted in Figs. 14 and 15), with significant implications for both packaging and cost. Although consideration of packaging and cost repercussions is beyond the scope of this paper the selection of the upper and lower limits of the motor/generator and battery size was such to meet the packaging requirement of this particular vehicle; namely, the vehicle could not accommodate bigger motor/generator size than 120 kW or bigger battery size than 10 modules.

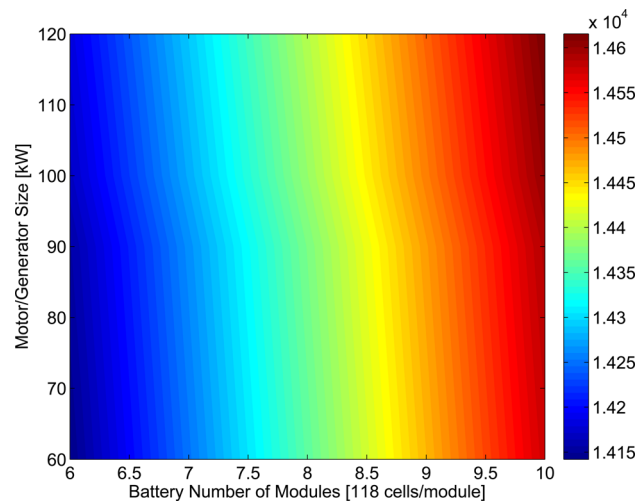


Fig. 14 Vehicle mass in kilograms (kg) for the PHEV pretransmission configuration

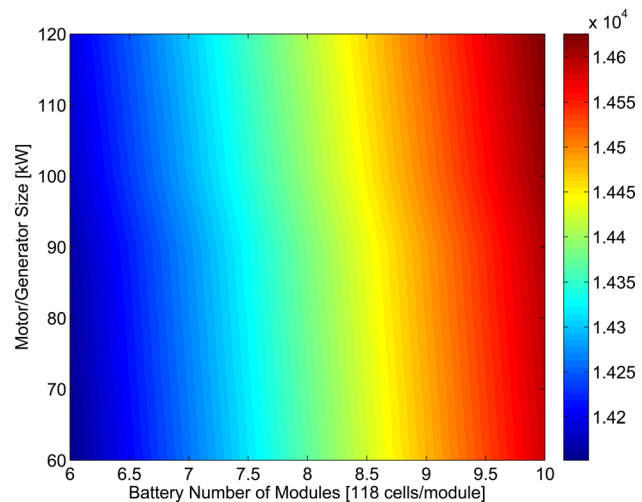


Fig. 15 Vehicle mass in kilograms (kg) for the PHEV post transmission configuration

5 Conclusion

We have demonstrated results using a proposed optimization framework to study the impact of motor/generator and battery size on fuel economy and GHG emissions of a medium duty PHEV. For the PHEV pretransmission configuration, it seems that there is a trade-off between fuel economy and GHG emissions when the motor/generator and battery size increases. However, in post transmission PHEV configurations, a combination of a big motor/generator size with a big battery size seems to be beneficial both in terms of fuel economy and GHG emissions as it enhances energy recovery during brake regeneration as a result of the physical location of the motor/generator.

The optimization and modeling approach adopted here facilitates better understanding of the potential benefits from proper selection of motor/generator and battery size. This understanding can help us identify the right sizing of these components, and thus reducing the PHEV cost. Addressing optimal sizing of PHEV components could aim to an extensive market penetration of PHEVs. Future research should consider the interactions between power management control strategies and these design variables. Simultaneous consideration of both design and power management may reveal more opportunities for substantial improvements in fuel economy and GHG emissions.

Acknowledgment

The author appreciates the insightful remarks and suggestions received from C. Stuart Daw and the assistance from David Smith with the Autonomie models. This research was supported by the U.S. Department of Energy. This support is gratefully acknowledged.

References

- [1] Lin, C.-C., Peng, H., Grizzle, J. W., and Kang, J.-M., 2003, "Power Management Strategy for a Parallel Hybrid Electric Truck," *IEEE Trans. Control Syst. Technol.*, **11**, pp. 839–849.
- [2] Pisu, P., and Rizzoni, G., 2007, "A Comparative Study of Supervisory Control Strategies for Hybrid Electric Vehicles," *IEEE Trans. Control Syst. Technol.*, **15**, pp. 506–518.
- [3] Sciarretta, A., Back, M., and Guzzella, L., 2004, "Optimal Control of Parallel Hybrid Electric Vehicles," *IEEE Trans. Control Syst. Technol.*, **12**, pp. 352–363.
- [4] Sciarretta, A., and Guzzella, L., 2007, "Control of Hybrid Electric Vehicles," *IEEE Control Syst. Mag.*, **27**, pp. 60–70.
- [5] Delprat, S., Lauber, J., Guerra, T. M., and Rimaux, J., 2004, "Control of a Parallel Hybrid Powertrain: Optimal Control," *IEEE Trans. Veh. Technol.*, **53**, pp. 872–881.
- [6] Antoniou, A. I., Komyathy, J., Bench, J., and Emadi, A., 2007, "Modeling and Simulation of Various Hybrid-Electric Configurations of the High-Mobility Multipurpose Wheeled Vehicle (HMMWV)," *IEEE Trans. Veh. Technol.*, **56**, pp. 459–465.
- [7] West, R. E., and Kreith, F., 2006, "A Vision for a Secure Transportation System Without Hydrogen or Oil," *ASME J. Energy Resour. Technol.*, **128**, pp. 236–243.
- [8] Himelc, J. B., and Kreith, F., 2011, "Potential Benefits of Plug-In Hybrid Electric Vehicles for Consumers and Electric Power Utilities," *ASME J. Energy Resour. Technol.*, **133**, pp. 031001–031006.
- [9] Gong, Q., Li, Y., and Peng, Z.-R., 2008, "Trip-Based Optimal Power Management of Plug-In Hybrid Electric Vehicles," *IEEE Trans. Veh. Technol.*, **57**, pp. 3393–3401.
- [10] Johannesson, L., Asbogard, M., and Egardt, B., 2007, "Assessing the Potential of Predictive Control for Hybrid Vehicle Powertrains Using Stochastic Dynamic Programming," *IEEE Trans. Intell. Transp. Syst.*, **8**, pp. 71–83.
- [11] Khaligh, A., Miraoui, A., and Garret, D., 2009, "Special Section on Vehicular Energy-Storage Systems," *IEEE Trans. Veh. Technol.*, **58**, pp. 3879–3881.
- [12] Wirasingha, S. G., and Emadi, A., 2011, "Classification and Review of Control Strategies for Plug-In Hybrid Electric Vehicles," *IEEE Trans. Veh. Technol.*, **60**, pp. 111–122.
- [13] Samaras, C., and Meisterling, K., 2008, "Life Cycle Assessment of Greenhouse Gas Emissions From Plug-In Hybrid Vehicles: Implications for Policy," *Environ. Sci. Technol.*, **42**, pp. 3170–3176.
- [14] Guzzella, L., and Amstutz, A., 1999, "CAE Tools for Quasi-Static Modeling and Optimization of Hybrid Powertrains," *IEEE Trans. Veh. Technol.*, **48**, pp. 1762–1769.
- [15] Wang, L., Collins, E. G., Jr., and Li, H., 2011, "Optimal Design and Real-Time Control for Energy Management in Electric Vehicles," *IEEE Trans. Veh. Technol.*, **60**, pp. 1419–1429.
- [16] Sung Chul, O., 2005, "Evaluation of Motor Characteristics for Hybrid Electric Vehicles Using the Hardware-in-the-Loop Concept," *IEEE Trans. Veh. Technol.*, **54**, pp. 817–824.
- [17] Inoa, E., and Wang, J., 2011, "PHEV Charging Strategies for Maximized Energy Saving," *IEEE Trans. Veh. Technol.*, **60**, pp. 2978–2986.
- [18] Tara, E., Shahidinejad, S., Filizadeh, S., and Bibeau, E., 2010, "Battery Storage Sizing in a Retrofitted Plug-In Hybrid Electric Vehicle," *IEEE Trans. Veh. Technol.*, **59**, pp. 2786–2794.
- [19] Trigger, L., Paterson, J., and Drozd, P., 1993, "Hybrid Vehicle Engine Size Optimization," SAE Future Transportation Technology Conference and Exposition, San Antonio, TX, SAE Paper No. 931793.
- [20] Aceves, S. M., Smith, J. R., Perkins, L. J., Haney, S. W., and Flowers, D. L., 1996, "Optimization of a CNG Series Hybrid Concept Vehicle," SAE International Congress and Exposition, Detroit, MI, SAE Paper No. 960234.
- [21] Moore, T., 1996, "Tools and Strategies for Hybrid-Electric Drivesystem Optimization," SAE Future Transportation Technology Conference and Exposition, Vancouver, Canada, SAE Paper No. 961660.
- [22] Zoelch, U., and Schroeder, D., 1998, "Dynamic Optimization Method for Design and Rating of the Components of a Hybrid Vehicle," *Int. J. Veh. Des.*, **19**, pp. 1–13.
- [23] Assanis, D., Delagrammatikas, G., Fellini, R., Filipi, Z., Liedtke, J., Michelena, N., Papalambros, P., Reyes, D., Rosenbaum, D., Sales, A., and Sasena, M., 1999, "An Optimization Approach to Hybrid Electric Propulsion System Design," *Mech. Struct. Mach.*, **27**(4), pp. 393–421.
- [24] Fellini, R., Michelena, N., Papalambros, P., and Sasena, M., 1999, "Optimal Design of Automotive Hybrid Powertrain Systems," Proceedings First International Symposium on Environmentally Conscious Design and Inverse Manufacturing, Los Alamitos, CA, Feb. 1–3, pp. 400–405.
- [25] Shiau, C. S. N., Kaushal, N., Hendrickson, C. T., Peterson, S. B., Whitacre, J. F., and Michalek, J. J., 2010, "Optimal Plug-In Hybrid Electric Vehicle Design and Allocation for Minimum Life Cycle Cost, Petroleum Consumption, and Greenhouse Gas Emissions," *ASME J. Mech. Des.*, **132**, p. 091013.
- [26] Yusaf, T. F., 2009, "Diesel Engine Optimization for Electric Hybrid Vehicles," *ASME J. Energy Resour. Technol.*, **131**, p. 012203.
- [27] Crane, D. T., and Bell, L. E., 2009, "Design to Maximize Performance of a Thermoelectric Power Generator With a Dynamic Thermal Power Source," *ASME J. Energy Resour. Technol.*, **131**, p. 0124011.
- [28] Gurkaynak, Y., Khaligh, A., and Emadi, A., 2009, "State of the Art Power Management Algorithms for Hybrid Electric Vehicles," 5th IEEE Vehicle Power and Propulsion Conference, VPPC '09, Dearborn, MI, Sept. 7–10, pp. 388–394.
- [29] Bumby, J. R., and Forster, I., 1987, "Optimisation and Control of a Hybrid Electric Car," *IEE Proc.-D: Control Theory Appl.*, **134**, pp. 373–387.
- [30] Capata, R., and Lora, M., 2007, "The LETHE Gas Turbine Hybrid Prototype Vehicle of the University of Roma 1: Drive Cycle Analysis of Model Vehicle Management Unit," *ASME J. Energy Resour. Technol.*, **129**, pp. 107–116.
- [31] Filipi, Z. S., Louca, L. S., Daran, B., Lin, C.-C., Yildir, U., Wu, B., Kokkolaras, M., Assanis, D. N., Peng, H., Papalambros, P. Y., and Stein, J. L., 2004, "Combined Optimization of Design and Power Management of the Hydraulic Hybrid Propulsion System for a 6 × 6 Medium Truck," *Heavy Vehicle Sys., Int. J. Vehicle Des.*, **11**(3–4), pp. 372–402.
- [32] Wu, L., Wang, Y., Yuan, X., and Chen, Z., 2011, "Multiobjective Optimization of HEV Fuel Economy and Emissions Using the Self-Adaptive Differential Evolution Algorithm," *IEEE Trans. Veh. Technol.*, **60**, pp. 2458–2470.
- [33] Nino-Baron, C. E., Tariq, A. R., Zhu, G., and Strangas, E. G., 2011, "Trajectory Optimization for the Engine-Generator Operation of a Series Hybrid Electric Vehicle," *IEEE Trans. Veh. Technol.*, **60**, pp. 2438–2447.
- [34] Syed, F. U., Kuang, M. L., Smith, M., Okubo, S., and Ying, H., 2009, "Fuzzy Gain-Scheduling Proportional-Integral Control for Improving Engine Power and Speed Behavior in a Hybrid Electric Vehicle," *IEEE Trans. Veh. Technol.*, **58**, pp. 69–84.
- [35] Solano Martinez, J., Hissel, D., Pera, M.-C., and Amiet, M., 2011, "Practical Control Structure and Energy Management of a Testbed Hybrid Electric Vehicle," *IEEE Trans. Veh. Technol.*, **60**, pp. 4139–4152.
- [36] Sezer, V., Gokasan, M., and Bogosyan, S., 2011, "A Novel ECMS and Combined Cost Map Approach for High-Efficiency Series Hybrid Electric Vehicles," *IEEE Trans. Veh. Technol.*, **60**, pp. 3557–3570.
- [37] Malikopoulos, A. A., and Smith, D. E., 2011, "An Optimization Model for Plug-In Hybrid Electric Vehicles," Proceedings of 2011 Fall Technical Conference of the ASME Internal Combustion Engine Division, Morgantown, WV, pp. 739–748.
- [38] Himelc, J. B., and Kreith, F., 2011, "Potential Benefits of Plug-In Hybrid Electric Vehicles for Consumers and Electric Power Utilities," *ASME J. Energy Resour. Technol.*, **133**(3), p. 031001.
- [39] Songqing, S., and Wang, G. G., 2010, "Metamodeling for High Dimensional Simulation-Based Design Problems," *J. Mech. Des.*, **132**, p. 051009.
- [40] Astrom, K. J., and Wittenmark, B., 1995, *Adaptive Control: Second Edition*, Addison Wesley Longman Publishing Co., Boston.
- [41] US Environmental Protection Agency, 2005, "Average Carbon Dioxide Emissions Resulting from Gasoline and Diesel Fuel," Office of Transportation and Air Quality, EPA420-F-05-00, http://www.epa.com/content-files/EPA_emissions_calc_420f05001.pdf, accessed on March, 2011.
- [42] Weber, C. L., Jaramillo, P., Marriott, J., and Samaras, C., 2010, "Life Cycle Assessment and Grid Electricity: What Do We Know and What Can We Know?," *Environ. Sci. Technol.*, **44**(6), pp. 1895–1901.
- [43] Hicks, C. R., and Turner, K. V., 1999, *Fundamental Concepts in the Design of Experiments*, 5th ed., Oxford University Press, New York.